21. R. Ghafouri, R. Bruinsma, *Phys. Rev. Lett.* **94**, 138101 (2005).

The Role of a Bilayer Interfacial Phase on Liquid Metal Embrittlement

Jian Luo,[1]* Huikai Cheng,[2] Kaveh Meshinchi Asl,[1] Christopher J. Kiely,[2] Martin P. Harmer[2]*

Intrinsically ductile metals are prone to catastrophic failure when exposed to certain liquid metals, but the atomic-level mechanism for this effect is not fully understood. We characterized a model system, a nickel sample infused with bismuth atoms, by using aberration-corrected scanning transmission electron microscopy and observed a bilayer interfacial phase that is the underlying cause of embrittlement. This finding provides a new perspective for understanding the atomic-scale embrittlement mechanism and for developing strategies to control the practically important liquid metal embrittlement and the more general grain boundary embrittlement phenomena in alloys. This study further demonstrates that adsorption can induce a coupled grain boundary structural and chemical phase transition that causes drastic changes in properties.

In liquid metal embrittlement (LME), intrinsically ductile metals, such as Al, Cu, and Ni, are prone to catastrophic brittle intergranular fracture at unusually low stress levels when exposed to certain liquid metals (*1*). LME can cause cracking during and/or after hot dip galvanizing or welding of steels and other nonferrous structural alloys. Furthermore, understanding LME is important for enabling the usage of liquid metals in the next generation of nuclear power generation systems and novel spallation target systems for nuclear waste incineration. In LME, the failure is known to originate at the grain boundaries (GBs), where the adsorption of the liquid metal element occurs (*2–4*), but an exact understanding of the embrittlement mechanism at an atomic level has puzzled the materials and physics communities for over a century. We have charac-terized GBs in a model LME system, Ni-Bi, by using aberration-corrected high-angle annular dark-field (HAADF) scanning transmission electron microscopy (STEM). Our study suggests that the embrittlement in Ni-Bi is due to bilayer adsorption of Bi atoms at general (i.e., high-energy and low-symmetry) GBs.

In a broader context, observation of these bilayers in a simple metallic system (Ni-Bi) fills a knowledge gap to demonstrate the general existence of discrete nanoscale GB-stabilized phases (also called complexions; see Fig. 1) (*5*). Whereas the existence of surface phases is well established (*6*), the identification of GB analogs at internal interfaces offers a different perspective for solving a variety of outstanding scientific problems (*7*, *8*). The coexistence of multiple interfacial phases at GBs with markedly different

[1]School of Materials Science and Engineering, Center for Optical Materials Science and Engineering Technology, Clemson University, Clemson, SC 20634, USA. [2]Department of Materials Science and Engineering, Center for Advanced Materials and Nanotechnology, Lehigh University, Bethlehem, PA 18015, USA.

*To whom correspondence should be addressed. E-mail: mph2@lehigh.edu (M.P.H.); jluo@alum.mit.edu (J.L.)
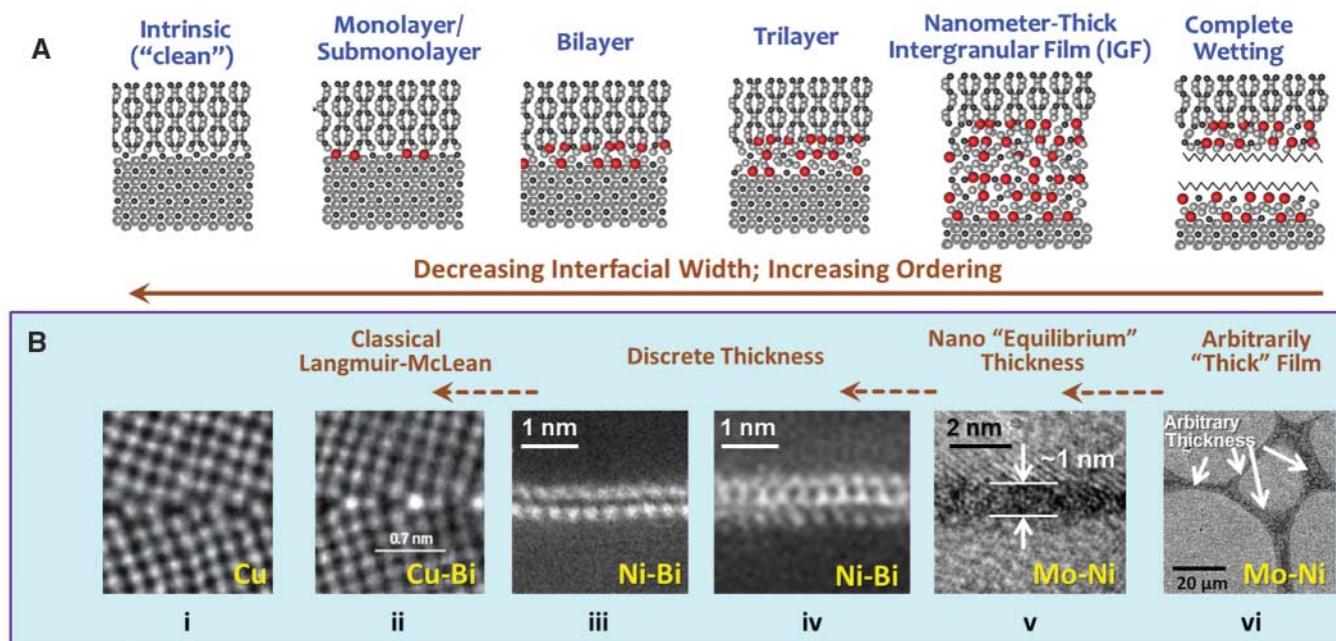
Fig. 1. (**A**) Six distinct interfacial phases have been observed in alumina and termed GB complexions (*7*, *8*). These schematics are adapted from (*7*) with permission. (**B**) Analogous interfacial phases in metals. The direct STEM HAADF observation of the most controversial bilayer and trilayer interfacial phases in a simple metal system, Ni-Bi, where the interpretation of images and their thermodynamic origin are less equivocal, authenticates the existence and generality of this series of generic interfacial phases. The physical origins of the nanoscale interfacial phases that are intermediate to the classical L-M adsorption and complete GB wetting are illustrated and discussed in the text. Micrographs i and ii are adapted from (*28*), and micrographs v and vi are adapted from (*11*) with permissions. Micrographs iii and iv are from the current work.

mobilities can lead to abnormal grain growth (8), and the enhanced diffusion in disordered GB phases can result in solid-state activated sintering (9). Classical theories recognize the existence of three distinct interfacial phases at GBs: namely, intrinsic (clean) GBs, Langmuir-McLean (L-M)

monolayer (or submonolayer) adsorption, and complete GB wetting films (Fig. 1). More recent high-resolution transmission electron microscopy (HRTEM) studies revealed the existence of impurity-containing intergranular films (IGFs) of equilibrium thickness in various ceramics

(10) and metals (9, 11) (Fig. 1B), as well as at metal-ceramic interfaces (12). The thermodynamic stability of these nanoscale IGFs can be explained from a balance of various interfacial forces (10, 12, 13) and by making analogies to the well-established surface premelting (14) and prewetting (15) theories (10, 16). If GB and surface adsorptions are indeed analogous, one may also expect that, in certain systems, interfacial phases can take on discrete thicknesses, leading to the formation of distinct bilayer and trilayer interfacial phases (Fig. 1) (17). The development of aberration-corrected STEM enabled us to resolve such ultrathin interfacial phases in a simple metallic system, Ni-Bi.

We isothermally annealed Ni foils in contact with Ni-Bi liquids (of equilibrium compositions) and quenched these specimens for characterization; the materials and methods used are described in supporting online material (SOM). Figures 2 and 3 summarize our key observations. Bi-Ni liquid penetrated substantially into the Ni GBs after annealing at 700° or 1100°C; in front of the micrometer-thick liquid penetration tips (referred to as micrometer-scale tips below; see Fig. 3B for an example), a characteristic bilayer interfacial phase (Fig. 2), which formed by GB diffusion of Bi, was found at nearly all GBs. This bilayer interfacial phase cannot be clearly discerned in conventional phase-contrast HRTEM (fig. S1). Energy-dispersive x-ray spectroscopy showed that these bilayers are Bi-enriched (fig.
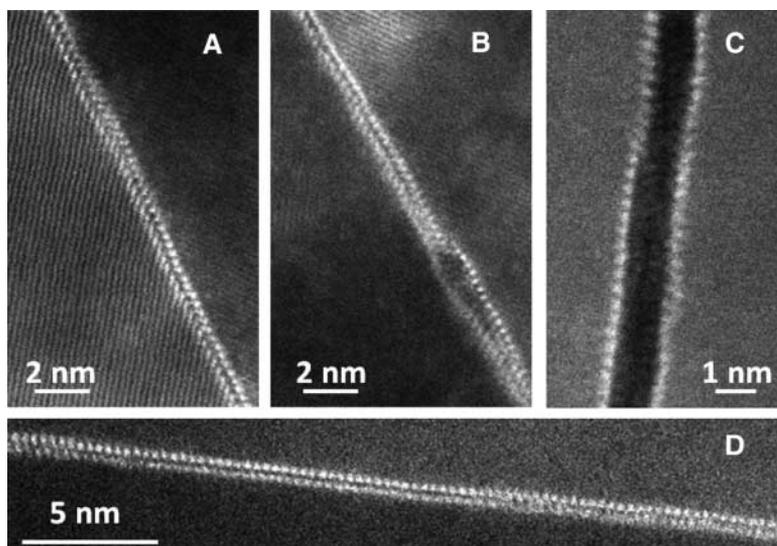
Fig. 2. (**A** and **B**) STEM HAADF micrographs showing two layers of Bi absorbed along the general GBs of a Ni polycrystal quenched from 700°C. (**C**) The weakly bonded Bi atoms could cause the boundaries to easily fracture between the layers and thus embrittle the material. Presumably, decohesion of this GB occurred during TEM specimen preparation. (**D**) This characteristic bilayer interfacial phase was also observed in specimens quenched from 1100°C.
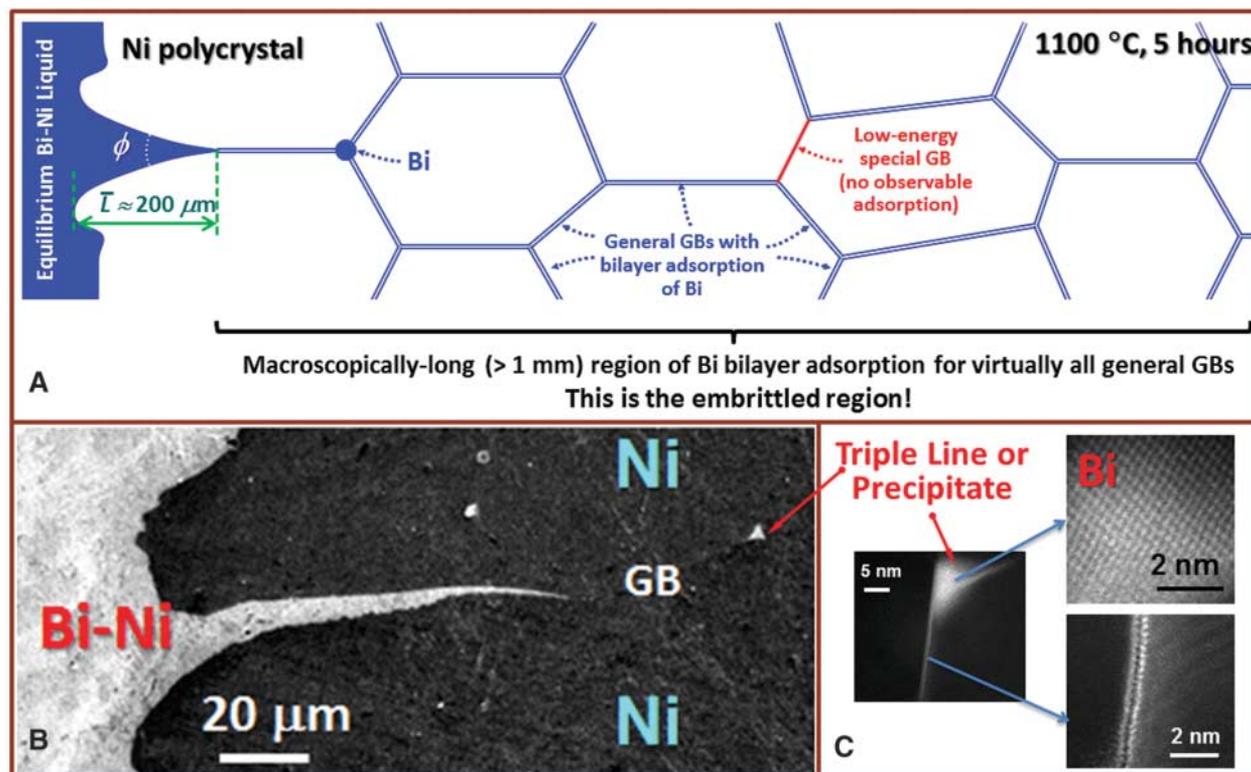
Fig. 3. Summary of the experimental observations for a specimen annealed at 1100°C for 5 hours. (**A**) A bilayer interfacial phase has been found at all independent general GBs examined in a prolonged embrittlement region in front of the micrometer-scale tips. (**B**) Scanning electron micrograph of a micrometer-scale tip. (**C**) STEM HAADF micrograph, showing the equilibrium among Ni grains, a Bi pocket, and a bilayer interfacial phase at the adjacent GB.

S2). Substantial efforts were made to exclude possible imaging artifacts (SOM and figs. S3 to S5). We refer to this interfacial phase as a bilayer because HAADF STEM images show that the adsorbed Bi atoms are primarily located within two atomic layers at GBs. As elaborated in the SOM, it is important to recognize that the GB excess of Bi is not necessarily identical to an equivalence of two monolayers of the bulk phase of pure Bi [using the definition of monolayer coverage adopted in prior studies (18–21)] because these bilayers do not exhibit the structure of any bulk phase (fig. S3) and are probably not pure Bi resulting from the effects of entropy-driven mixing.

For the specimens annealed at 1100°C for 5 hours, the average penetration length for the micrometer-scale tips was ~200 µm (Fig. 3B). The characteristic bilayer interfacial phase was observed at general GBs, not only near the micrometer-scale tips but also in locations that were about 1 mm away from the micrometer-scale tips (Fig. 3 and fig. S6). It was established that this macroscopic long region of constant Bi adsorption is the embrittled region (2, 3). The observed bilayer structures are essentially identical in STEM HAADF images, where the Bi atoms show up as bright spots by virtue of their higher atomic mass regardless of the annealing temperature (700° versus 1100°C), annealing time (1 to 5 hours), and the distance from the liquid front (~0 to >1 mm). This is indicative of a GB "phase" behavior, where the phase-defining variables take on discrete values.

Seven independent, flat, edge-on GBs were examined in this study, out of which only one did not show bilayer Bi adsorption (SOM and figs. S6 to S9). Further examination using electron backscatter diffraction showed that this "clean" GB is in fact a low-angle GB (fig. S7), and GB adsorption is less likely to occur at special low-energy GBs. Furthermore, one of the GBs that we examined was composed of multiple facets, and bilayers were observed at all six faceted segments that could be clearly imaged (fig. S8). This further supports the proposition that bilayers are the representative interfacial phase under this condition. The bilayers were also found in the GBs directly adjacent to the wetted triple lines or Bi precipitates (Fig. 3C and fig. S10), indicating that this bilayer interfacial phase must be in equilibrium with the two adjoining bulk phases.

These bilayers are largely ordered in STEM HAADF images (Fig. 2). Specifically, the STEM HAADF image in fig. S3 shows that each of the Bi layers is adsorbed coherently on the adjacent Ni grain, but there is no lattice-matching relation between the two adsorbed Bi layers. A proposed model for these bilayers is shown in fig. S11b. This is consistent with prior modeling work, which showed that the adjacent crystal would impose some structural order that decays exponentially with a decaying length on the order of one interatomic distance (22, 23). Thus, the series of interfacial phases shown in Fig. 1 should exhibit

increasing levels of structural order with decreasing interfacial width, and bilayers should be substantially more ordered than IGFs of 1 to 2 nm thick.

The formation of this bilayer interfacial phase can be understood via the following thought experiment. In the presence of liquid Bi species, a general GB in Ni would be "separated" into two grain surfaces, each with a monolayer surface adsorption of Bi (coherently on the Ni grain surface as shown in fig. S3), which are only weakly bonded to each other (incoherently; fig. S3). Such a bilayer interfacial phase can be energetically favored because Bi atoms bond strongly to Ni atoms on the grain surface and Bi-Bi bonds are easier to break (SOM and fig. S11). In contrast, a monolayer is likely to be energetically more expensive to form at a general GB (with no lattice-matching relation between the two grain surfaces) because one of the Ni-Bi interfaces must be incoherent, which requires breaking some of the stronger Ni-Bi bonds (fig. S11a).

We also observed a trilayer interfacial phase (Fig. 1 and fig. S12). Only a single observation of such a trilayer was made (at a portion of GB that was immediately adjacent to a micrometer-scale tip), indicating that it may represent a metastable

interfacial phase [the formation of which could be stimulated by a local tensile stress generated by the liquid metal penetration (24)]. Nonetheless, the coexistence of two distinct interfacial phases at one GB (fig. S12) indicates the existence of an interfacial phase transition between them.

Although the series of six generic conformations of interfacial phases shown in Fig. 1A have been identified in alumina containing various dopants (7, 8), the validity and generality of these interfacial phases are under scrutiny (5). The existence and generality of the bilayer and trilayer interfacial phases are the most controversial (5). Specifically, the interaction of an atomic step and a monolayer adsorption can give rise to the illusion of a bilayer in the projected image. As shown in fig. S4, we verified that the bilayer in Ni-Bi was authentic by performing a series of careful through-focus imaging experiments. Furthermore, although a trilayer-like structure has been implicated by conventional HRTEM of a special GB in a Ga-implanted Al specimen (25), the present STEM HAADF observation of the trilayer interfacial phase in a general GB provides evidence for its natural existence. Lastly, the STEM HAADF observation of the bilayer and trilayer interfacial phases in a simple metallic sys-
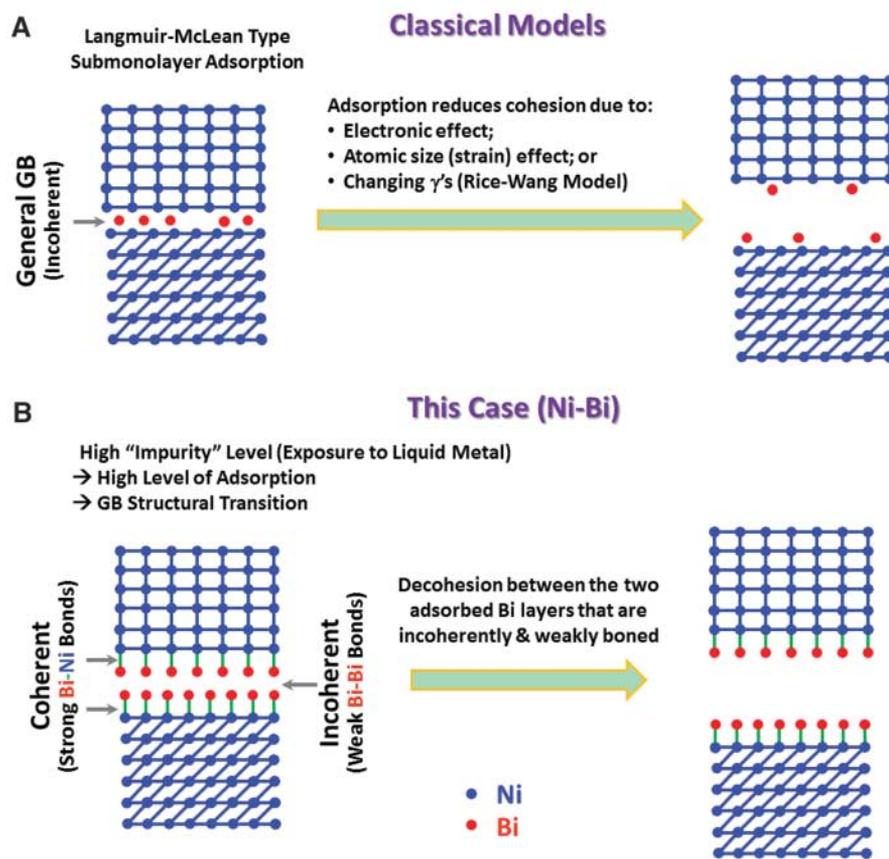
Fig. 4. (A) All three classical GB embrittlement models were built on the traditional L-M type adsorption model. (B) Our study of LME in Ni-Bi demonstrated that a high adsorption level can induce a GB structural and chemical transition to form a new bilayer interfacial phase, which more drastically reduces the GB cohesion. The proposed bilayer structure is supported by the HAADF STEM image analysis shown in fig. S3, and the model is shown in fig. S11.

tem, where the possible interpretation of their origin will be considerably less controversial than that for complex ceramic systems like alumina, helps establish a systematic picture of the interfacial phase behaviors (Fig. 1) (5, 8).

In the 1970s, Hondros and Seah (26) were the first to propose a model for multilayer GB adsorption based on an analogy of the well-known Brunauer-Emmett-Teller surface adsorption model (which did not predict discrete interfacial phases). In the past 4 decades, GB compositional measurements suggested the possible existence of multilayer adsorption in several systems, most notably in Cu-Bi (27); however, the estimated adsorption levels vary from submonolayer (2, 18, 20, 28) to ~2 monolayers (18, 27) to 1- to 4-nm-thick IGFs (4). In Ni-Bi, although a simple auger electron spectroscopy (AES) estimation suggested the existence of a monolayer to bilayer adsorption transition (29), more quantitative AES measurements of specimens prepared under virtually identical conditions as those used in the present study suggested the existence of 2- to 3-nm Bi-containing IGFs (2, 3). In contrast, the current study using HAADF STEM directly shows that this adsorption is better described as (~0.7-nm-thick) bilayers.

To understand the embrittlement mechanism, we can consider LME as an especially severe case of GB embrittlement, which occurs at high impurity levels. In classical metallurgy, the GB adsorption of impurities can lead to a drastic loss of mechanical strength, but important controversies persist regarding the mechanisms of this GB embrittlement phenomenon (28, 30–32). The three classical GB embrittlement models were all built on the traditional L-M GB adsorption model, where the reduction of GB cohesion was explained from either an electronic effect (28, 31), an atomic size difference (strain) effect (30), or the changes in relative interfacial energies (the Rice-Wang model) (33) (Fig. 4A). As a starting point, the reduction of GB cohesion resulting from the bilayer adsorption may be explained by the Rice-Wang model (33) with modifications, where the embrittlement should be more severe than that for a case of L-M GB adsorption because of a greater amount of adsorption (Fig. 4B). However, the Rice-Wang model does not consider that an adsorption-induced GB structural transition can more drastically change the properties. Specifically in our case, the average (projected) distance between two neighboring Bi columns from the opposing layers is 0.39 nm (fig. S13); this implies that the distance between the neighboring Bi atoms in the opposite layers in three dimensions should be greater than 0.39 nm, which is considerably greater than the bulk Bi-Bi metallic bond length of 0.353 nm. Thus, the interlayer Bi-Bi bonds are likely lengthened and thus weakened. From the STEM images, we cannot completely rule out the possibility that there is a Ni layer between the two adsorbed Bi layers that is not visible in STEM HAADF and that embrittlement of GBs is thusly related to the brittleness of the intermetallic compound; however, the analysis presented in fig.

S11c shows that such an interfacial structure is likely unstable at a general GB because it implies the existence of an incoherent Ni-Bi interface. In any case, our study suggests that the bilayer interfacial phase at general GBs is implicated for LME.

Our observation demonstrates that adsorption can induce a coupled GB structural and chemical phase transition, leading to abrupt changes in properties (embrittlement in this case). A recent atomistic simulation (32) of a model GB embrittlement system Ni-S suggested that S adsorption causes embrittlement by inducing a GB structural transition (amorphization). Indeed, nanoscale "amorphous" IGFs have been observed by HRTEM for two GB embrittlement systems: W-Ni (9) and Mo-Ni (11) (Fig. 1). These results, along with the current study of Ni-Bi as the most direct example, collectively point us to revisit the traditional GB embrittlement models to consider nonclassical GB segregation associated with the formation of an interfacial "phase" beyond the traditional L-M adsorption.

References and Notes

1. B. Joseph, M. Picat, F. Barbier, *Eur. Phys. J. Appl. Phys.* **5**, 19 (1999).
2. K. Wolski, V. Laporte, *Mater. Sci. Eng. A* **495**, 138 (2008).
3. N. Marié, K. Wolski, M. Biscondi, *Scr. Mater.* **43**, 943 (2000).
4. K. Wolski, V. Laporte, N. Marié, M. Biscondi, *Interface Sci.* **9**, 183 (2001).
5. M. P. Harmer, *Science* **332**, 182 (2011).
6. R. Pandit, M. Schick, M. Wortis, *Phys. Rev. B* **26**, 5112 (1982).
7. S. J. Dillon, M. Tang, W. C. Carter, M. P. Harmer, *Acta Mater.* **55**, 6208 (2007).
8. M. P. Harmer, *J. Am. Ceram. Soc.* **93**, 301 (2010).
9. V. K. Gupta, D. H. Yoon, H. M. Meyer III, J. Luo, *Acta Mater.* **55**, 3131 (2007).
10. J. Luo, *Crit. Rev. Solid State Mater. Sci.* **32**, 67 (2007).
11. X. Shi, J. Luo, *Appl. Phys. Lett.* **94**, 251908 (2009).
12. M. Baram, D. Chatain, W. D. Kaplan, *Science* **332**, 206 (2011).
13. D. R. Clarke, *J. Am. Ceram. Soc.* **70**, 15 (1987).
14. J. G. Dash, A. M. Rempel, J. S. Wettlaufer, *Rev. Mod. Phys.* **78**, 695 (2006).
15. J. W. Cahn, *J. Chem. Phys.* **66**, 3667 (1977).
16. M. Tang, W. C. Carter, R. M. Cannon, *Phys. Rev. Lett.* **97**, 075502 (2006).
17. J. Luo, *Appl. Phys. Lett.* **95**, 071911 (2009).
18. V. J. Keast, A. La Fontaine, J. du Plessis, *Acta Mater.* **55**, 5149 (2007).
19. Y.-M. Chiang, H. Wang, J.-R. Lee, *J. Microsc.* **191**, 275 (1998).
20. U. Alber, H. Mullejans, M. Rühle, *Acta Mater.* **47**, 4047 (1999).
21. J. A. S. Ikeda, Y.-M. Chiang, A. J. Garratt-Reed, J. B. V. Sande, *J. Am. Ceram. Soc.* **76**, 2447 (1993).
22. A. Hashibon, J. Adler, M. W. Finnis, W. D. Kaplan, *Comput. Mater. Sci.* **24**, 443 (2002).
23. Y. Kauffmann et al., *Acta Mater.* **59**, 4378 (2011).
24. L. Klinger, E. Rabkin, *Scr. Mater.* **62**, 918 (2010).
25. W. Sigle, G. Richter, M. Rühle, S. Schmidt, *Appl. Phys. Lett.* **89**, 121911 (2006).
26. E. D. Hondros, M. P. Seah, *Metall. Trans.* **8A**, 1363 (1977).
27. L.-S. Chang et al., *Scr. Metall. Mater.* **37**, 729 (1997).
28. G. Duscher, M. F. Chisholm, U. Alber, M. Rühle, *Nat. Mater.* **3**, 621 (2004).
29. L. S. Chang, K. B. Huang, *Scr. Mater.* **51**, 551 (2004).
30. R. Schweinfest, A. T. Paxton, M. W. Finnis, *Nature* **432**, 1008 (2004).
31. M. Yamaguchi, M. Shiga, H. Kaburaki, *Science* **307**, 393 (2005); 10.1126/science.1104624.
32. H. P. Chen et al., *Phys. Rev. Lett.* **104**, 155502 (2010).
33. J. R. Rice, J.-S. Wang, *Mater. Sci. Eng. A* **107**, 23 (1989).

Efficient Dehydrogenation of Formic Acid Using an Iron Catalyst

Albert Boddien,[1,2] Dörthe Mellmann,[1] Felix Gärtner,[1] Ralf Jackstell,[1] Henrik Junge,[1] Paul J. Dyson,[2] Gábor Laurenczy,[2]* Ralf Ludwig,[3]* Matthias Beller[1]*

Hydrogen is one of the essential reactants in the chemical industry, though its generation from renewable sources and storage in a safe and reversible manner remain challenging. Formic acid (HCO_2H or FA) is a promising source and storage material in this respect. Here, we present a highly active iron catalyst system for the liberation of H_2 from FA. Applying 0.005 mole percent of $Fe(BF_4)_2 \cdot 6H_2O$ and tris[(2-diphenylphosphino)ethyl]phosphine [$P(CH_2CH_2PPh_2)_3$, PP_3] to a solution of FA in environmentally benign propylene carbonate, with no further additives or base, affords turnover frequencies up to 9425 per hour and a turnover number of more than 92,000 at 80°C. We used in situ nuclear magnetic resonance spectroscopy, kinetic studies, and density functional theory calculations to explain possible reaction mechanisms.

Hydrogen is of critical importance in the chemical industry and might play a key role in the future in renewable energy technologies. As a potential secondary energy vector it would enable clean energy storage and transduction. If H_2 is combusted in engines or fuel cells, only water emerges as benign exhaust (1–3). Although synthetic catalytic transformations of hydrogen mainly rely on expensive, low-abundant precious metal catalysts (4, 5), iron-based enzymes efficiently metabolize H_2 as an energy source in many organisms. For